American Mineralogist, Volume 83, pages 823–834, 1998

The influence of water on the structure of hydrous sodium tetrasilicate glasses

Nikolay Zotov[1,2,*] and Hans Keppler[1]

[1]Bayerisches Geoinstitut, Universität Bayreuth, Bayreuth 95440, Germany
[2]Central Laboratory of Mineralogy and Crystallography, Bulgarian Academy of Sciences, Rakovski str. 92, Sofia 1000, Bulgaria

Abstract

The structure of sodium tetrasilicate ($Na_2Si_4O_9$) glasses containing 0 to 10 wt% water was investigated by a combination of Raman, IR, and NMR methods. Both the ^{29}Si magic angle spinning NMR data and Raman spectra in the Si-O stretching region clearly show that water depolymerizes the silicate network of the glasses. Q-species distributions calculated from Raman spectra, assuming equal scattering cross sections of all bands in the Si-O stretching region, closely agree with results obtained from NMR data. At low total water contents, the silicate network is depolymerized mainly by breaking of Q^4-Q^4 bonds, whereas breaking of Q^3-Q^3 bonds dominates at high water contents. Near IR spectra show the presence of both OH groups and molecular H_2O in the glasses. The number of nonbridging O atoms per silicon atom, calculated from the near IR data, closely agrees with the results obtained from Raman and NMR, and confirms the assignment of the 4500 cm^{-1} band in the near IR to a combination mode of Si-OH groups. Moreover, the intensity of the fundamental Si-OH stretching band at 910 cm^{-1} in the Raman spectra varies proportionally to the intensity of the 4500 cm^{-1} near IR band. Both IR and Raman spectra show three main bands in the OH-stretching region, centered at 3580, 3000, and 2350 cm^{-1}, due to hydrous species with different hydrogen bond strengths. The relative intensities of these three bands are insensitive to total water content and OH/H_2O ratio, suggesting that both OH and H_2O contribute to each of these bands. This is consistent with the fine structure of the H_2O bending vibration in the IR spectra around 1640 cm^{-1} and with the polarization dependence of the OH-stretching bands in the Raman spectra. Near IR spectra of hydrous sodium tetrasilicate glasses and hydrous aluminosilicate glasses are very similar and show a similar dependence of band intensity on total water content, suggesting that there is no fundamental difference in the dissolution mechanism of water in these systems.

Introduction

Water is the most important volatile component in natural magmas. Accordingly, considerable effort has been expanded over several decades to understand the dissolution mechanism of water in silicate melts (McMillan 1994). In-situ spectroscopic measurements of hydrous silicate melts at high temperature and high pressure have only recently become feasible and are essentially still limited to near IR and Raman techniques (e.g., Keppler and Bagdassarov 1993; Nowak and Behrens 1995; Shen and Keppler 1995; Holtz et al. 1996). These measurements show that the structure of hydrous melt and quenched glass at room temperature are qualitatively similar. However, quantitative data on melt structure cannot be obtained from quenched samples, because speciation in hydrous glasses changes even below the glass transformation temperature (Nowak and Behrens 1995; Shen and Keppler 1995). Nevertheless, studies of hydrous glasses still provide a valuable first step toward understanding the dissolution of water in silicate melts. In particular, various spectroscopic and diffraction methods can be used simultaneously on glasses and the results can be cross-checked in order to establish proper procedures for the quantitative evaluation of spectroscopic data. Proper band assignments and structural models can then be used to study the structure of hydrous silicate melts directly at high pressure and high temperature.

Presently, even the structure and vibrational spectra of relatively simple hydrous silicate glasses are not sufficiently understood (McMillan 1994).Whereas a general consensus exists that both molecular H_2O and OH groups are present in hydrous glasses (Batholomew et al. 1980; Stolper 1982), different estimates of the OH/H_2O ratio are sometimes obtained from IR, Raman, and NMR data (Farnan et al. 1987; Eckert et al. 1987). Moreover, the structural role of OH in hydrous aluminoslicate glasses is still debated. Whereas some models invoke the formation of Si-OH or Al-OH groups, implying depolymerization of the glass structure by water (Burnham 1979; Sykes and Kubicki 1993), other models imply that water has no effect on the degree of polymerization (Kohn et al. 1989). Some of these discrepancies are related to disparate as-

* E-mail: Nikolay.Zotov@Uni-Bayreuth.De

0003–004X/98/0708–0823$05.00

signments of various bands in the near IR and Raman spectra of hydrous glasses (McMillan 1994). Also, the spatial relationship between OH and H_2O and the extent of hydrogen bonding for these species is poorly understood (e.g., Schaller and Sebald 1995).

The existing controversies appear to result from use of only one or two spectroscopic methods to investigate a system and to establish a structural model. Combining a wide variety of spectroscopic and diffraction methods will help to establish a coherent structural model of a simple binary hydrous alkalisilicate glass. This study combines previous results from neutron diffraction (Zotov et al. 1996), various NMR methods (Kümmerlen et al. 1992; Schaller and Sebald 1995), reverse Monte Carlo simulations (Zotov and Keppler 1998), with new Raman, IR, and ^{29}Si MAS NMR data to cross-check various spectroscopic methods and to establish proper band assignments in vibrational spectra. The system sodium tetrasilicate ($Na_2Si_4O_9$)-H_2O was examined because highly resolved ^{29}Si NMR spectra can be obtained (Kümmerlen et al. 1992), and the compositional simplicity facilitates peak assignments in vibrational spectra as well as in the radial distribution functions obtained from neutron diffraction (Zotov et al. 1996).

Experimental methods

Anhydrous sodium tetrasilicate ($Na_2Si_4O_9$) glass was prepared by melting homogenized mixtures of stoichiometric quantities of SiO_2 (analytical grade Merck) and Na_2CO_3 (analytical grade Merck) in a platinum crucible at 1200 °C for about 20 h and quenching the crucible in water. The final composition (20.5 mol% Na_2O, 79.5 mol% SiO_2) was measured by ICP-AES (inductively coupled plasma atomic emission spectrometry). Protonated and deuterated glasses were synthesized in a rapid-quench TZM-autoclave. For each experiment, appropriate amounts of anhydrous glass and deuterium oxide (99.8% D_2O, Heraeus) or doubly distilled water were loaded in platinum capsules (5 mm diameter, 3.5 cm length, 0.15 mm wall thickness) and hermetically sealed by arc-welding. The capsules were first compressed at 1 kbar and room temperature and then kept in a drying oven for 1 h. The weight of the capsules before and after this procedure was compared to detect any leaks. Only capsules without significant change in weight were used in the high-pressure synthesis. The capsules were then heated to 1100 °C under 2 kbar Ar pressure for 20 h and isobarically quenched to room temperature within 1–2 s.

The density of several samples was measured using a hydrostatic Berman balance with toluene as reference liquid and the results were averaged. The standard deviations are typically 0.05 g/cm^3. For the rest of the samples the densities were determined by linear interpolation. The total water content of all samples was measured at least two times by Karl-Fischer titration (Behrens et al. 1996).

All IR measurements were carried out using a Bruker IFS 120 HR Fourier-transform spectrometer. Absorption spectra in the near-IR (NIR) range from 3900 to 7500 cm^{-1} were measured using a Bruker IR microscope attached to the spectrometer. Measuring conditions were tungsten light source, CaF_2 beamsplitter, liquid N_2-cooled narrow-band mercury cadmium telluride (MCT) detector, 4 cm^{-1} resolution, and 100 scans per sample. Doubly polished plates with about 450 μm thickness were used. The thickness was measured with a micrometer to ±2 μm. Some measurements were also carried out on thinner plates; all peaks in the near IR scaled directly proportional to the thickness of the samples, implying that they represent species dissolved in the glass and are not due to surface-absorbed material. Moreover, the spectra were independent of the time the samples had been stored in a desiccator. Mid-IR (MIR) absorption spectra from 600 to 4000 cm^{-1} were acquired using a globar source, a KBr beamsplitter, and an MCT detector. There were 200 scans with 1 cm^{-1} resolution for each sample. Samples were either very thin (10–15 μm) doubly polished plates or KBr-pellets. IR absorption spectra in the far-IR (FIR) range from 150 to 700 cm^{-1} were measured in the evacuated sample chamber of the spectrometer with a mercury discharge lamp, 3.5 μm Mylar beamsplitter, DTGS detector, 2.0 cm^{-1} resolution, and 400–1000 scans per sample. Both doubly polished plates with 10–50 μm thickness and polyethylene pellets were used.

Raman spectra were measured in 155° scattering geometry with the 514.5 nm line of a Coherent Ar^+ ion laser, a SPEX 1877 triplemate spectrometer and a Photometrics CCD camera cooled by liquid N_2. Wavenumbers were calibrated against the lines of an Ne discharge lamp. Resolution is about 4 cm^{-1}. Spectra were measured on the same doubly polished plates as used for the NIR measurements. High-quality data were acquired by overlapping spectral windows, each covering approximately 400 cm^{-1} with accumulation times of typically from 10 to 60 min per scan and about 1.0 W laser power at the sample. The Raman spectra measured in different spectral windows were first converted into counts per minute, Fourier smoothed, rebinned with constant step of $\Delta\nu = 1$ cm^{-1} using a spline interpolation and then merged together using a least-squares procedure. The measurement of absolute Raman intensities is very difficult (Long 1977). Therefore, we have normalized the Raman spectra, requiring that the integrated area in the range 100–1200 cm^{-1} equals 1000. These first-order Raman spectra $I_N(\nu)$ were then corrected for frequency and temperature effects using the expression:

$$I_R(\nu) = \nu[1 - \exp(-h\nu c/kT)]I_N(\nu)/(\nu_0 - \nu)^4 \quad (1)$$

where h is the Plank's constant, c is the speed of light, k is the Boltzmann constant, and ν_0 is the wavenumber of the incident laser light (Long 1977). Polarized (VV and VH) spectra were recorded using a dichroic sheet polarizer (Melles Griot) in the scattered beam. The accuracy $\Delta\rho$ of the depolarization ratio $\rho = I_{VH}/I_{VV}$ was estimated to be $\Delta\rho = \pm 0.02$ by measuring the A_1 fundamental vibration of CCl_4 liquid at about 460 cm^{-1} (Long 1977).

All ^{29}Si MAS NMR spectra were recorded on a Bruker

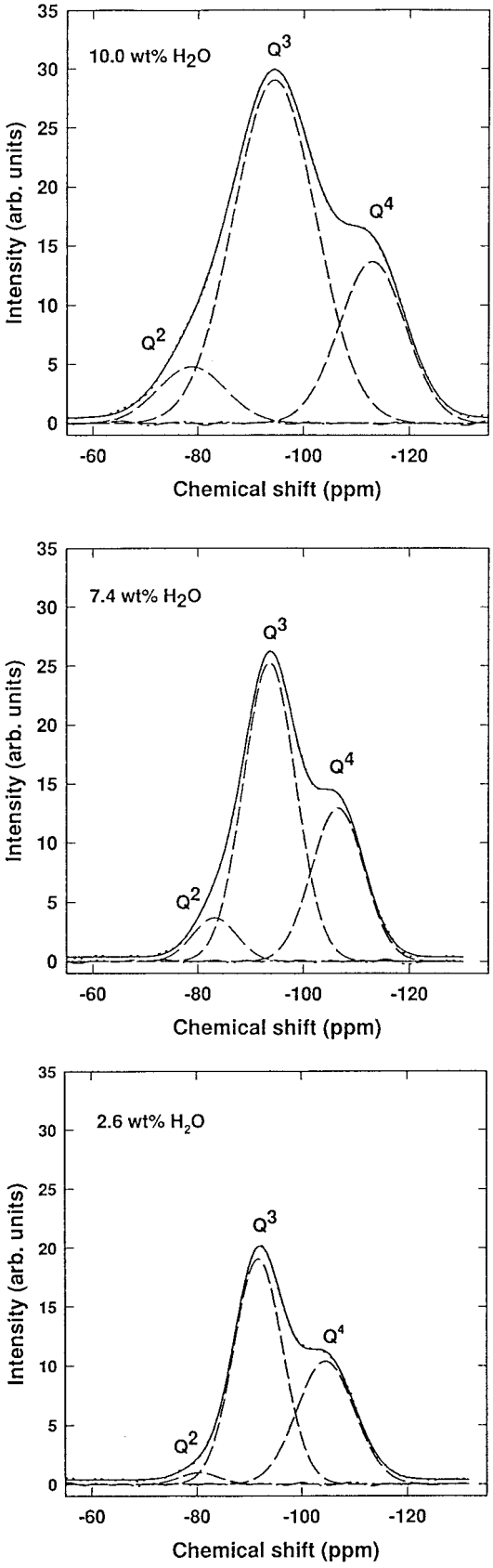

FIGURE 1. ^{29}Si MAS NMR spectra of hydrous sodium tetrasilicate glasses with 2.6, 7.4, and 10.0 wt% total water. Experimental data (dotted line), fit (full line), difference (dash-dotted line), individual bands (dashed lines).

→

MSL 300 or MSL 200 (samples with 2.6 and 7.3 wt% total water) NMR spectrometer with a spinning frequency of 4 kHz. Pulse length was 2.5 μs with a relaxation delay of 30 s. These conditions were checked and found appropriate for quantification purposes (Kümmerlen et al. 1992). In particular, measurements with variable relaxation delay ranging from 15 to 240 s yielded no significant variation in the shape or intensity of the spectra, demonstrating the absence of differential relaxation (J. Kümmerlen, personal communication). For high signal-to-noise ratios, up to 6000 scans were accumulated using 200 mg of powdered sample. No apodization or baseline correction was carried out. The ^{29}Si chemical shifts of all samples are reported relative to TMS (tetramethylsilane). The total area of the spinning sidebands was only about 6.5% of the intensity in the center of the spectrum; therefore, the sidebands were not considered in the quantification of the spectra. Additional experimental details and complementary NMR data will be discussed elsewhere (Schaller et al., in preparation).

RESULTS AND DISCUSSION

Q-species distribution

The structure of the silicate network in a glass is mainly determined by the degree of polymerization of the silicate tetrahedra and described by the abundance of different Q^n species, where Q^n denotes a tetrahedron linked by bridging O atoms to n adjacent tetrahedra. The range of n is 0 (isolated tetrahedra) to 4 (fully polymerized three-dimensional network). Anhydrous $Na_2Si_4O_9$ glass contains 0.5 Na ions per Si, thus on the average only one O atom in every second tetrahedron is saturated by Na and not available for bridging two tetrahedra. Accordingly, one would expect that dry $Na_2Si_4O_9$ glass contains about 50% Q^3 and about 50% Q^4 species in close agreement with ^{29}Si MAS NMR measurements (Dupree et al. 1984; Emerson et al. 1989; Maekawa et al. 1991). The effect of water on the Q-species distribution can be monitored both by ^{29}Si MAS NMR spectroscopy and by Raman measurements in the Si-O stretching region around 1100 cm^{-1}. However, whereas obtaining the Q-species distribution from ^{29}Si NMR data are rather straightforward, controversies remain regarding the assignment of Raman peaks (McMillan 1994).

Representative ^{29}Si NMR spectra of hydrous sodium tetrasilicate glasses (Fig. 1) were decomposed into three Gaussian components centered at about −80, −93, and −104 ppm that directly give the abundance of the Q^2, Q^3, and Q^4 species (Engelhardt and Michel 1987). The precise peak position, band width, and intensity were not constrained in the fitting procedure. Excellent fits were

TABLE 1. Q-species distribution from ^{29}Si MAS NMR experiments

H_2O (wt%)	Q^2 (%)	Q^3 (%)	Q^4 (%)	Ref.
0.0	0.0	48.0	52.0	[1]
2.62 ± 0.05*	2.4 ± 0.5	59.8 ± 0.4	37.8 ± 0.3	this study
4.80	3.0	66.0	30.0	[1]
7.34 ± 0.45*	7.6 ± 0.2	62.0 ± 0.4	30.4 ± 0.2	this study
9.1	17.0	63.0	19.0	[1]
10.0 ± 0.35*	8.9 ± 0.4	66.2 ± 0.5	24.9 ± 0.4	this study

Note: [1] = Kümmerlen et al. 1992. The errors in the Q-species are calculated from the least-squares decomposition.
* Determined by Karl-Fischer titration.

obtained for all samples with goodness-of-fit factors of about 1%. Q-species distributions (Table 1) are consistent with those of Kümmerlen et al. (1992), except for the high abundance of Q^2 species in their sample with 9.1 wt% water. Because the abundance of Q^2 units in all other samples is low, their apparent high concentration could result from noise in the spectra. Due to larger amounts of sample and longer accumulation times, the signal/noise ratio of our measurements is much better than in the previous study (Kümmerlen et al. 1992), which may explain the apparent discrepancy. Another source of error could be the fitting procedure of Kümmerlen et al. (1992), wherein almost pure Gaussian profiles were used for Q^3 and Q^4 components, but a Gauss-Lorentz mixture was used for Q^2 resonance, although there is little theoretical justification for doing this. Accordingly, we suspect that the Q^2 abundance reported for the sample with 9.1 wt% water may be unrealistically high.

VV and VH polarized Raman spectra are given in Figure 2. To determine the Q-species distribution, the reduced unpolarized (VV+VH) spectra were fitted with Gaussian components, although in some cases a slight improvement of the fit could be achieved using pseudo-Voigt functions. Rather than determining statistically in each case the optimum number of bands that could be fitted (Mysen et al. 1982a), we have used a fitting model with a fixed number of Gaussians centered at about 800, 900, 950, 1040, 1100, and 1140 cm^{-1} (Fig. 3). Very good fits were obtained with goodness-of-fit factors ranging from 1.8 to 3.4%. This approach is justified by near independence of positions of the high-frequency bands in alkali and alkaline-earth silicate glasses from the degree of polymerization and the type of the network modifier (Mysen et al. 1982b). The peak near 950 cm^{-1} is usually assigned to Si-O stretching vibrations in Q^2 units and the principal peak at about 1100 cm^{-1} Si-O stretching vibrations of in Q^3 units (Brawer and White 1975; Furukawa et al. 1981; Mysen et al. 1982b; Matson et al. 1983; McMillan 1984). There is some controversy on the origin of the 1140 and 1040 cm^{-1} bands (see McMillan 1984 for discussion). Our preferred assignment (Zotov and Keppler 1997) is that the 1140 cm^{-1} band originates from symmetric Si-O stretching vibrations in Q^4 species whereas the 1040 cm^{-1} band originates from Q^3 species (denoted hereafter $Q^{3'}$) distinct from those responsible for the 1100 cm^{-1} band (denoted hereafter $Q^{3''}$). If one further assumes that the scattering cross sections for all the bands mentioned are equal, i.e., that the integral band intensity is directly proportional to the abundance of the respective Q-species, the Q-species distributions obtained for all samples are in close agreement with the results from the NMR data (Table 2 and Fig. 4).

With increasing water content, the abundance of Q^4 units in the glass clearly decreases (Fig. 4). The structure of the glass is thus depolymerized by water, presumably by formation of SiOH groups from bridging O atoms according to the equation:

$$Si - O - Si + H_2O \rightarrow Si - OH + HO - Si. \quad (2)$$

The formation of Si-OH groups has been associated with the appearance of a new peak around 900 cm^{-1} in hydrous silicate and alumosilicate glasses, although assignment of this peak to Si-OH groups has been questioned

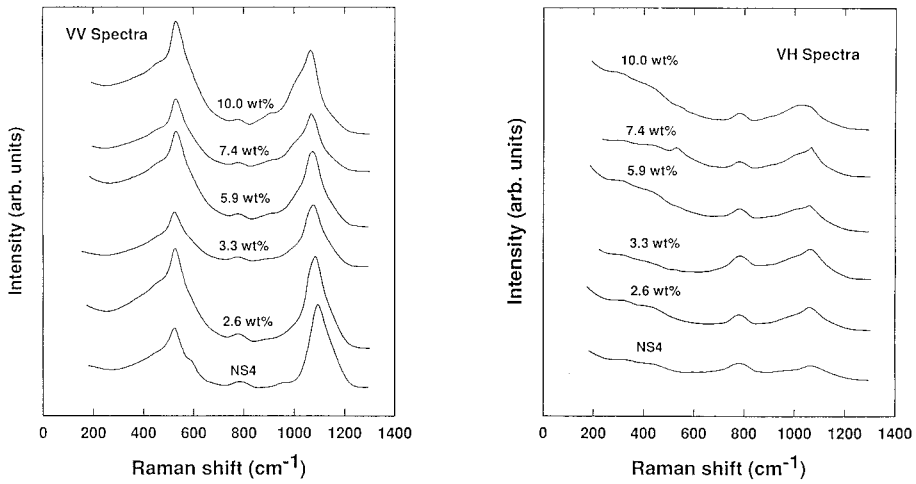

FIGURE 2. Polarized (VV and VH) Raman spectra of hydrous sodium tetrasilicate glasses.

(see McMillan et al. 1993 for discussion). We observe a new weak peak at about 910 cm^{-1} in the polarized (VV and VH) spectra of the hydrous sodium tetrasilicate glasses (Figs. 2 and 3), with a depolarization ratio of 0.35 ± 0.12. Its integral intensity increases with increasing total water content up to 6 wt% (Fig. 5) and then levels off and is accompanied by a slight increase in frequency.

The 910 cm^{-1} band in the hydrous sodium tetrasilicate glasses exhibits a small negative isotopic shift of about 20 cm^{-1} (ν_H/ν_D = 1.022), whereas the remaining Raman bands in the Si-O stretching region are not affected by deuteration. This isotopic shift resembles the value expected for a simple harmonic oscillator ($\nu_H/\nu_D = (M_{OD}/M_{OH})^{0.5} = (18/17)^{0.5} = 1.029$). Much smaller isotopic shifts ν_H/ν_D = 1.004 for the band close to 900 cm^{-1} have been observed in hydrous aluminosilicate glasses (Mysen et al. 1980; Mysen and Virgo 1986; McMillan et al. 1993) and used to argue against assigning this band to Si-OH vibrations (or Al-OH vibrations in alumosilicate glasses). The small isotopic shift in hydrous albite glasses was tentatively explained by McMillan et al. (1993) on the basis of the Redlich-Teller product rule. Because the strength of the vibrational coupling (respectively the degree of delocalization of the vibrational modes) should decrease with depolymerization, this effect should be weaker in hydrous tetrasilicate than in hydrous feldspar glasses. This is consistent with the larger isotopic shift observed in our study and therefore supports the interpretation of McMillan et al. (1993) that the band around 900 cm^{-1} is indeed due to Si-OH or Al-OH vibrations.

Water also strongly effects on the Raman spectra of the sodium tetrasilicate glasses around 600 and 800 cm^{-1}. The polarized peak at about 600 cm^{-1} is usually assigned to planar three-membered rings (Kubicki and Sykes 1993; Zotov et al. 1993 and references therein). This peak decreases in intensity in the hydrous glasses and disappears completely above 3 wt% total water (Fig. 2). The presence of a relatively large number of three-membered rings in the structure of the anhydrous sodium tetrasilicate glass was confirmed by reverse Monte Carlo simulations (Zotov and Keppler 1998). The Si-O-Si bond angle in planar three-membered rings is 130.5° (Galeener 1982), which corresponds to very high-strain energy (Newton and Gibbs 1980), and therefore these bonds would be the first in the silicate network to react with water. The changes in the rest of the polarized Si-O-Si and O-Si-O bending modes in the range 200–700 cm^{-1} (depolarization ratios 0.08–0.15) are much more subtle.

The integral intensity of the band at about 800 cm^{-1} (Fig. 2), decreases rapidly with increasing water content up to 6 wt% after which levels off (Fig. 5). According to preliminary calculations of Raman spectra (Zotov and Keppler, in preparation), this band arises from cage-like vibrations of Si atoms mainly in Q^4-tetrahedra. The decrease of this band therefore directly reflects the disruption of the three-dimensional network structure of the glass.

The frequencies of all major Raman bands are nearly independent of water content, except that the 1100 cm^{-1} component slightly decreases with water (Fig. 6). The mid-IR and far-IR spectra below 1200 cm^{-1} are generally similar to the Raman spectra, with comparable variations with water content. Because the bands in the IR spectra are generally broader and show less fine structure, these IR results are not discussed further.

Depolymerization mechanism

Below about 3.5 wt% total water, the Q^4 species in the glass matrix decrease, whereas the Q^3 units increase correspondingly and the Q^2 units are hardly affected (Fig. 4). This suggests that water initially reacts with the O atoms bridging two Q^4 units according to $Q^4 - Q^4 \rightarrow Q^3 + Q^3$. In this low water content regime, the Q^3 units are essentially not attacked by water, although they initially occur in the glass with approximately the same abundance as the Q^4 species. This situation changes above 6 wt% total water. Here, the abundance of Q^4 units remains constant whereas the Q^2 species slowly increase at the expense of Q^3. This suggests that water reacts with O atoms bridging two Q^3 tetrahedra according to $Q^3 - Q^3 \rightarrow Q^2 + Q^2$. For intermediate compositions (3.5 to 6 wt% total water), the $Q^4 - Q^3 \rightarrow Q^3 + Q^2$ and $Q^3 - Q^3 \rightarrow Q^2 + Q^2$ mechanisms compete.

The above depolymerization mechanisms can be rationalized by strain-energy considerations. Reverse Monte Carlo simulations (Zotov and Keppler 1998) of the structure of the anhydrous sodium tetrasilicate glass revealed that the Q^4-O-Q^4 bridges have an asymmetric bond angle distribution with a maximum at about 120° (Fig. 7) and mean value 133° ± 16°, whereas the Q^4-O-Q^3 distribution is more symmetric with mean value at about 138° ± 16° and the Q^3-O-Q^3 distribution is bimodal with maxima at about 125 and 165°, respectively. The dependence of the potential energy of the Si_2O_7 dimer on the Si-O-Si bond angle (Newton and Gibbs 1980) implies that the Q^4-O-Q^4 bonds have a larger strain energy than the Q^4-O-Q^3 or Q^3-O-Q^3 species. Therefore, water would initially react with the O atoms in Q^4-O-Q^4 bridges, leading to an increase of the Q^3 species and corresponding decrease of the Q^4 species. This explains the observed changes in the Q-species distribution at low-water content and suggests that the changes in the depolymerization mechanism at higher-water content are also related to changes in the bond-angle distribution of the different Q^i-O-Q^j species.

Water speciation

The concentrations of molecular H_2O and of OH groups in silicate glasses can be determined from the combination bands in the near IR spectra (Batholomew et al. 1980; Stolper 1982). The 5250 cm^{-1} band is commonly assigned to the combination mode of the stretching and bending vibrations of the H_2O molecule. The 4500 cm^{-1} band is believed to be due to a combination of the O-H and Si-OH stretching vibrations of hydroxyl groups attached to Si. The 5250 and 4500 cm^{-1} bands, as well as the band at about 4000 cm^{-1}, are superimposed on a

FIGURE 3. Examples of unpolarized Raman spectra of hydrous sodium tetrasilicate glasses in the Si-O stretching region (700–1300 cm^{-1}). Experimental data (dotted line), fit (full line), difference (dash-dotted line), individual bands (dashed lines). The difference curves are offset by 0.5 units for clarity.

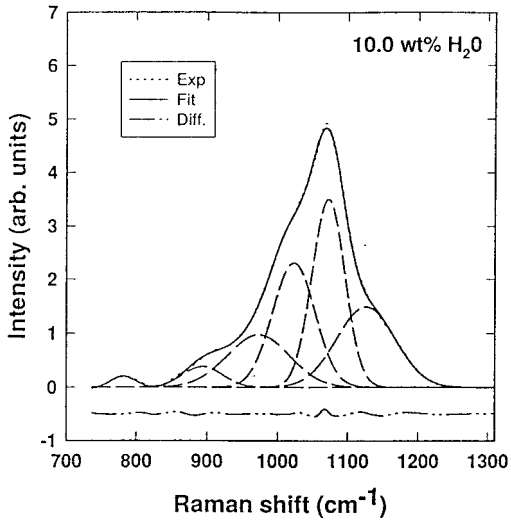

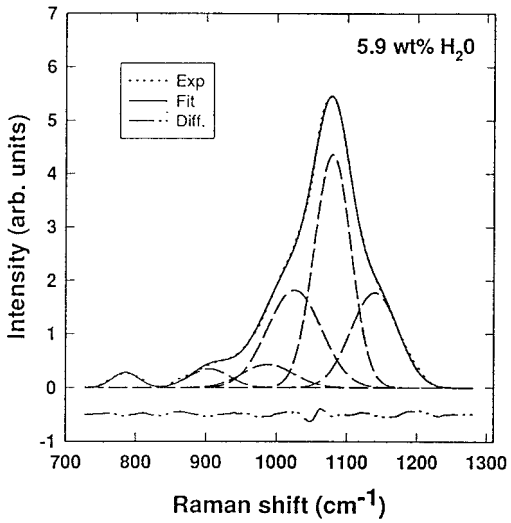

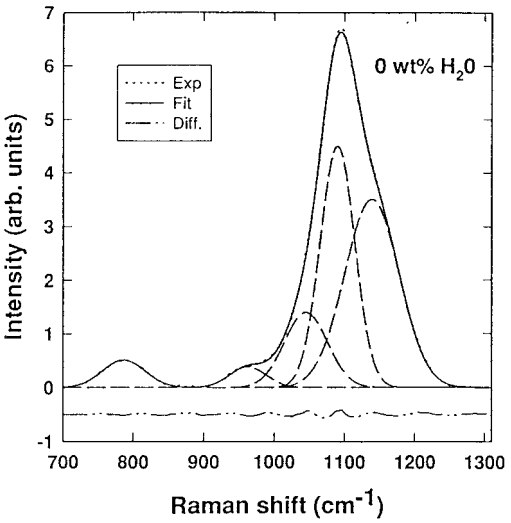

non-linear background that represents the tail of the O-H fundamental at about 3600 cm^{-1}. To correct for this background, a spline-function was fitted through the points below 3800 cm^{-1}, the minima between the 4000, 4400, and 5250 cm^{-1} bands and the tail beyond 5500 cm^{-1} (Fig. 8). Integrated intensities A_{H_2O} and A_{OH} of the 5250 and 4500 cm^{-1} bands were determined by numerical integration. The percentage (in weight percent) of the water present as H_2O molecules and OH groups is related to the integral intensities A_{H_2O} and A_{OH} by the Lambert-Beer law:

$$c_{H_2O} = MA_{H_2O}/\rho t\epsilon_{H_2O} \quad (3)$$

$$c_{OH} = MA_{OH}/\rho t\epsilon_{OH} \quad (4)$$

where M is the molar weight of water (18.02 g/mol), ρ is the density of the glass, t is the thickness of the sample, and ϵ_{H_2O} and ϵ_{OH} are the corresponding integral molar extinction coefficients (in l/mol-cm^2) of H_2O and OH, respectively. Together with the relationship

$$c_{tot} = c_{H_2O} + c_{OH} \quad (5)$$

where c_{tot} is the total water content, these equations can be combined to give

$$(tc_{tot}\rho)/(A_{OH}\ M) = 1/\epsilon_{OH} + (1/\epsilon_{H_2O})(A_{H_2O}/A_{OH}). \quad (6)$$

A least-squares fit to this equation (Fig. 9) yields integrated extinction coefficients of $\epsilon_{OH} = 56.0 \pm 6.9$ l/mol-cm^2 and $\epsilon_{H_2O} = 146.8 \pm 19.0$ l/mol-cm^2. The fact that the data for all glasses can be fitted to a straight line without significant deviation from linearity implies that the extinction coefficients are constant over the concentration range studied. The integral extinction coefficient of the H_2O band is about two times the value for OH; a similar ratio was reported by Acocella et al. (1984) for linear extinction coefficients in hydrous sodium trisilicate glasses. With these extinction coefficients, the concentrations of OH groups and molecular H_2O were calculated (Fig. 10 and Table 3). At low concentrations, water is mostly dissolved as OH groups in the glass, whereas at high water contents molecular H_2O dominates. Similar behavior has been reported for various hydrous silicate glasses (e.g., Bartholomew et al. 1980; Stolper 1982; Acocella et al. 1984).

The shape of the OH band at 4500 cm^{-1} is almost symmetric, but the H_2O band (5250 cm^{-1}) has a long asymmetric tail extending down to 4750 cm^{-1}. Asymmetric shapes were reported also by Langer and Flörke (1974), Stolper (1982), Behrens et al. (1996), Yanev and Zotov (1996), and others. The origin of the asymmetry of the 5250 cm^{-1} band and the true profile shape are still not

TABLE 2. Relative integral intensities of Raman bands and corresponding Q-species distribution

H_2O (wt%)*	I_{Q2}†	I_{Q3}‡	I_{Q3}§	I_{Q4}#	Q^2 (%)**	Q^3 (%)**	Q^4 (%)**
0.0	24.1 ± 7.3	107.3 ± 5.4	285.0 ± 6.7	335.7 ± 4.4	3.2 ± 1.0	52.2 ± 2.0	44.6 ± 1.3
2.62 ± 0.05	28.0 ± 3.6	89.9 ± 5.0	296.7 ± 5.2	264.6 ± 3.8	4.1 ± 0.6	56.9 ± 1.8	39.0 ± 1.1
3.29 ± 0.16	32.9 ± 5.3	186.2 ± 7.5	310.4 ± 4.5	206.0 ± 3.2	4.5 ± 0.8	67.5 ± 2.2	28.0 ± 0.8
5.86 ± 0.17	52.5 ± 10.1	174.3 ± 8.7	284.6 ± 6.7	144.8 ± 3.2	8.0 ± 1.8	69.9 ± 3.3	22.1 ± 1.0
7.34 ± 0.45	61.1 ± 21.1	164.4 ± 25.2	241.4 ± 12.5	149.2 ± 2.5	9.9 ± 4.0	65.9 ± 8.3	24.2 ± 1.8
10.0 ± 0.35	88.8 ± 16.8	175.3 ± 16.6	220.2 ± 12.0	146.1 ± 2.6	14.1 ± 3.3	62.7 ± 5.9	23.2 ± 1.4

* Determined by Karl-Fischer titration.
† Intensity of the Raman band near 950 cm^{-1}.
‡ Intensity near 1040 cm^{-1}.
§ Intensity near 1100 cm^{-1}.
# Intensity near 1150 cm^{-1}.
** The standard deviations $\sigma(I_{Q2})$, $\sigma(I_{Q3})$, and $\sigma(I_{Q4})$ of the integral intensities are determined from the least-squares Gaussian fits: $\sigma(Q^2) = 100\{[\sigma(I_{Q2})A + I_{Q2}\,\sigma(A)]/A^2\}$; $\sigma(Q^3) = 100\{[\sigma(I_{Q3})A + I_{Q3}\,\sigma(A)]/A^2\}$; $\sigma(Q^4) = 100\{[\sigma(I_{Q4})A + I_{Q4}\,\sigma(A)]/A^2\}$, where A is the total area of the $Q^2 + Q^3 + Q^4$ bands and $\sigma(A)$ is the corresponding standard deviation, calculated by $\sigma^2(A) = \sigma^2(I_{Q2}) + \sigma^2(I_{Q3}) + \sigma^2(I_{Q4})$.

well understood. We have tentatively modeled the 5250 cm^{-1} band using slightly asymmetric Gauss function centered at about 5245 cm^{-1} and a second much broader Gauss function centered at about 5140 cm^{-1}. Except for the sample with 2.6 wt% total water, the intensity ratio of these two components is practically constant for all concentrations studied. This justifies the use of one single-integral molar extinction coefficient encompassing both components.

The IR band at 4500 cm^{-1} has been attributed to OH groups attached to a tetrahedral cation, i.e., Si or Al (Batholomew et al. 1980; Stolper 1982). However, this interpretation has been questioned on the basis of NMR data on hydrous aluminosilicate glasses (Kohn et al. 1989). Instead of forming Si-OH groups, water would be incorporated in the glass as molecular H_2O, OH groups attached to Na ions and protons attached to bridging O atoms (Kohn et al. 1989; Pichavant et al. 1992). The above data can quantitatively test assignment of the 4500 cm^{-1} band. The data on the Q-species distribution from NMR and Raman spectra (Tables 1 and 2), imply an average number on nonbridging O atoms per Si:

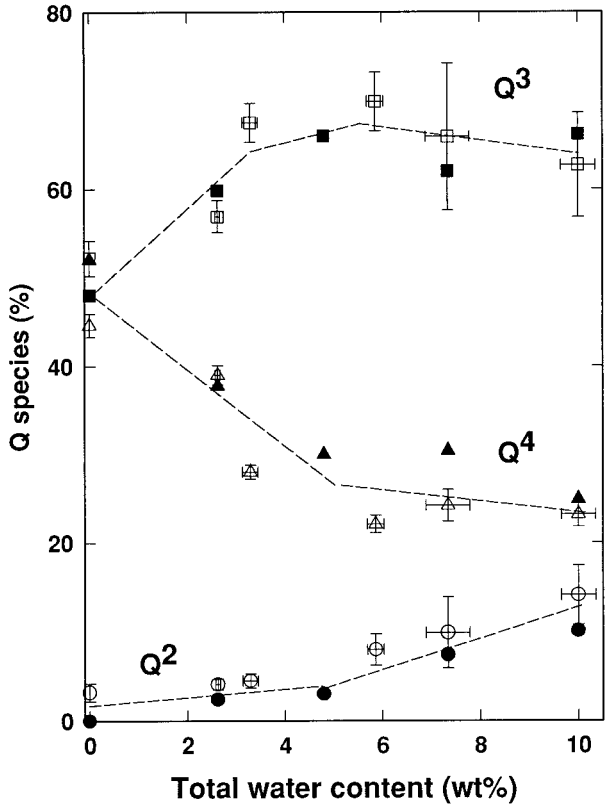

FIGURE 4. Dependence of the Q-species distribution in hydrous sodium tetrasilicate glasses on the total water content: Q^2 (circles), Q^3 (squares), Q^4 (triangles). Raman data (open symbols), NMR data (filled symbols). The dashed lines are only a guide for the eyes.

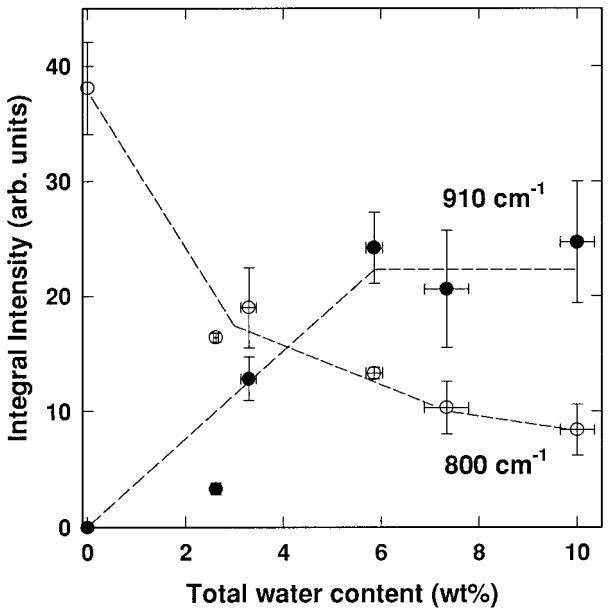

FIGURE 5. Integral intensity of the 800 (open circles) and 910 (filled circles) cm^{-1} band in the reduced unpolarized Raman spectra as function of total water content. The dashed lines are a guide for the eyes only.

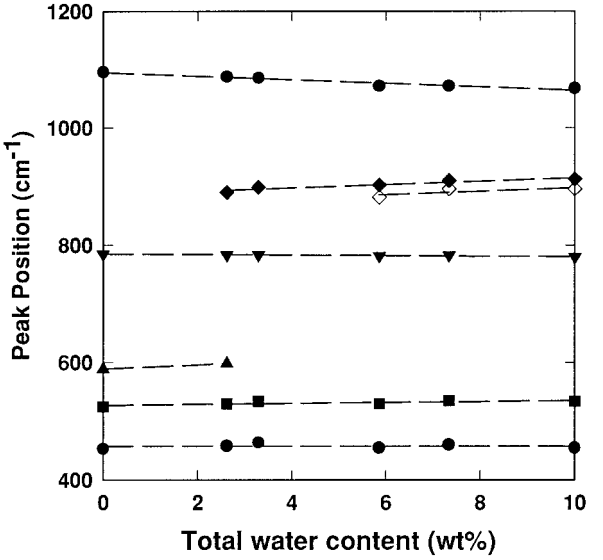

FIGURE 6. Peak positions of the principal Raman bands as function of total water content. Protonated samples (full symbols), deuterated samples (empty symbols). The dashed lines are linear regression fits.

$$\text{NBO/Si} = \Sigma\ (4 - n)x_n \qquad (7)$$

where x_n is the fraction of Q^n species in the glass (normalized to $\Sigma\ x_n = 1$). An independent measure of NBO/Si is obtained from Table 3, assuming that the OH content derived from the intensity of the 4500 cm^{-1} band is exclusively due to Si-OH groups. With this assumption, every OH will generate one additional NBO/Si, starting with an average NBO/Si of 0.5 for the anhydrous glass. These two calculations are in perfect agreement (Fig. 11), confirming that the combination band at 4500 cm^{-1} is

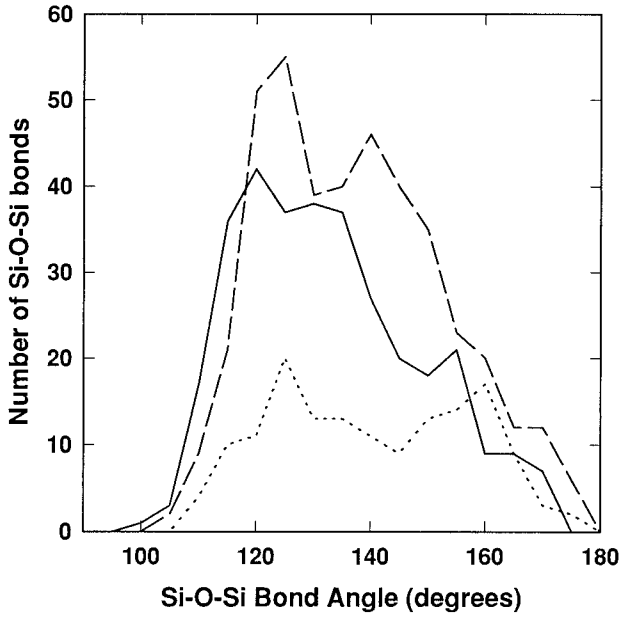

FIGURE 7. Distribution of Si-O-Si bond angles for different Q^i-O-Q^j species according to a model of the anhydrous sodium tetrasilicate glass obtained by reverse Monte Carlo simulations: Q^4-O-Q^4 (full line), Q^4-O-Q^3 (dashed line), Q^3-O-Q^3 (dotted line).

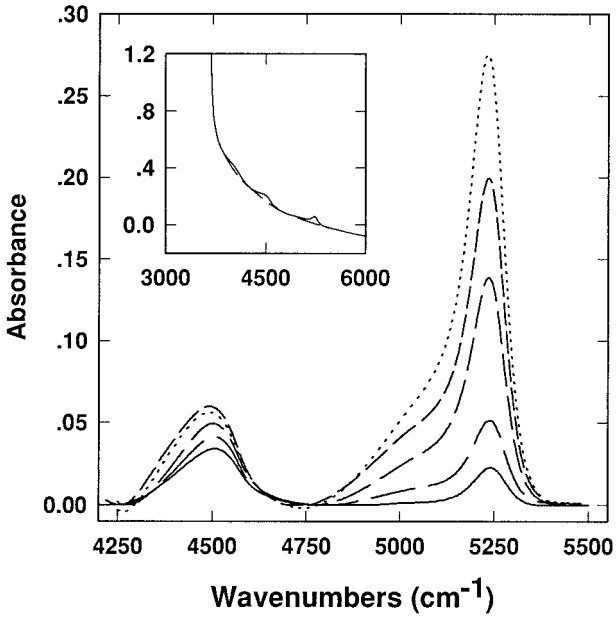

FIGURE 8. Baseline-corrected near IR spectra of hydrous sodium tetrasilicate glasses with 2.62 wt% total water (full line), 3.29 wt% (long-dash line), 5.86 wt% (medium-dash line), 7.34% (short-dash line) and 10.0 wt% (dotted line). All spectra are normalized to 450 μm thickness. The inset shows the raw spectrum (full line) of the sample with 3.29 wt% total water together with background (dashed line).

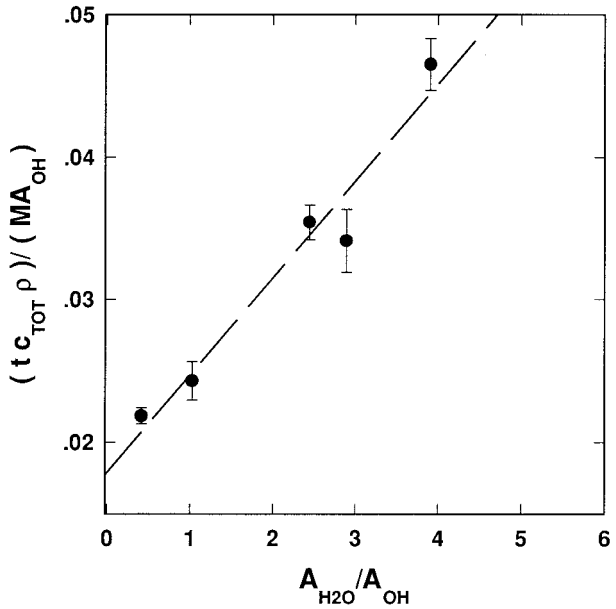

FIGURE 9. Plot of $(tc_{TOT}\rho)/MA_{OH}$ vs. the ratio of the integral absorbances A_{H_2O}/A_{OH}. The dashed line is a linear regression fit.

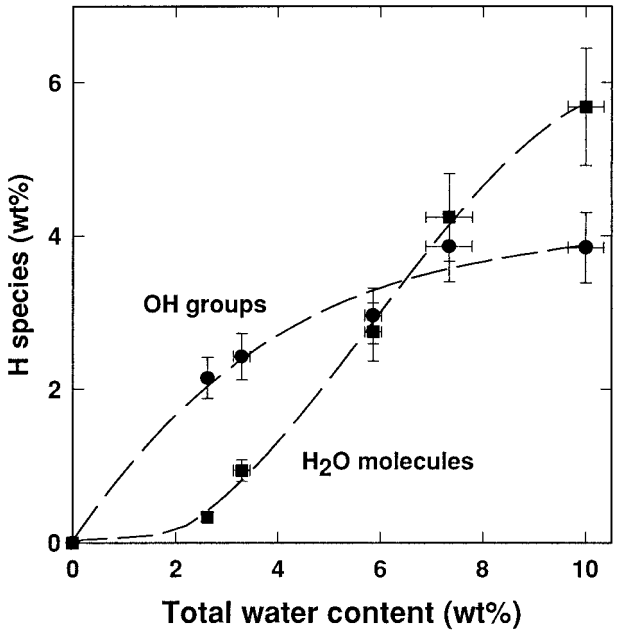

FIGURE 10. Dependence of the concentration of OH groups and H_2O molecules in hydrous sodium tetrasilicate glasses on the total water content. The dashed lines are a guide for the eyes only.

really due to Si-OH groups and that insignificant amounts of Na-OH species or protons attached to bridging O atoms are present. The same conclusion was reached by Kümmerlen et al. (1992) based on $^1H \rightarrow {}^{29}Si$ cross polarization NMR experiments. Moreover, comparison of Figures 5 and 9 shows that the intensity of the Si-OH band in the Raman spectra at about 910 cm^{-1} varies proportionally to the abundance of OH groups as derived from the 4500 cm^{-1} band in the near IR spectra. All these observations, together with the isotopic shift of the 910 cm^{-1} band upon deuteration, establish beyond any reasonable doubt that both the 910 cm^{-1} band and the 4500 cm^{-1} band are due to vibrations of Si-OH groups.

Hydrogen bonding

Whereas the near IR spectra provide information on the relative abundance of OH groups and molecular H_2O, the effects of different hydrogen bond strengths can be seen in the fundamental OH stretching region of the IR and Raman spectra (Figs. 12 and 13). The three well-resolved peaks at 3580, 3000, and 2350 cm^{-1} correspond to hydrous species (OH or H_2O) with OH···O distances of 3, 2.7, and 2.55 Å, respectively (Nakamoto et al. 1955). All distances have uncertainties of ±0.05 Å. The species responsible for the 3580 cm^{-1} band experience almost no hydrogen bonding, whereas the 2350 cm^{-1} band is due to some structural units with strong hydrogen bonding. The relative intensities of the three bands differ between the Raman and IR spectra, due to the well-known effect of hydrogen-bonding on IR extinction coefficients (Pimental and McClellan 1960; Paterson 1982; Buback et al. 1987). With increasing hydrogen bonding, i.e., decreasing stretching frequency, IR extinction coefficients increase by orders of magnitude, whereas Raman scattering cross sections are hardly affected (Scherer 1978; Buback et al. 1987). Accordingly, the Raman spectra in Figure 13 probably give a more direct picture of the relative abundance of the various species. Thus, the units with strong hydrogen bonding (2350 cm^{-1} band) make up only about 3% of the hydrous species, whereas the weekly hydrogen bonded species (3580 cm^{-1} band) represent 25%. Upon deuteration, all three main bands shift to lower frequency (Fig. 14). The frequency ratio ν_{OH}/ν_{OD} for the 3580 cm^{-1} band is between 1.35 and 1.38 and is between 1.28 and 1.34 for the 3000 cm^{-1} band.

TABLE 3. Water speciation in hydrous sodium tetrasilicate glasses

Total water (wt%)*	c_{OH} (wt%)†	c_{H_2O} (wt%)‡	c_{TOT} (wt%)§
2.62 ± 0.05	2.15 ± 0.27	0.34 ± 0.06	2.49 ± 0.28
3.29 ± 0.16	2.42 ± 0.30	0.95 ± 0.14	3.37 ± 0.33
5.86 ± 0.17	2.96 ± 0.36	2.75 ± 0.37	5.71 ± 0.52
7.34 ± 0.45	3.86 ± 0.46	4.24 ± 0.57	8.10 ± 0.74
10.0 ± 0.35	3.85 ± 0.46	5.68 ± 0.76	9.53 ± 0.89

* Determined by Karl-Fischer titration.
† $\sigma(c_{OH}) = K[A_{OH}\sigma(1/\epsilon_{OH}) + \sigma(A_{OH})(1/\epsilon_{OH})]$.
‡ $\sigma(c_{H_2O}) = K[A_{H_2O}\,\sigma(1/\epsilon_{H_2O}) + \sigma(A_{H_2O})(1/\epsilon_{H_2O})]$.
§ $c_{TOT} = c_{OH} + c_{H_2O}$; $\sigma^2(c_{TOT}) = \sigma^2(c_{OH}) + \sigma^2(c_{H_2O})$, where K = 18.02/pt and $\sigma(1/\epsilon_{OH})$, $\sigma(1/\epsilon_{H_2O})$, σ_{Aoh} and σ_{Ah_2o} are the corresponding standard deviations of the extinction coefficients and the integral NIR intensities.

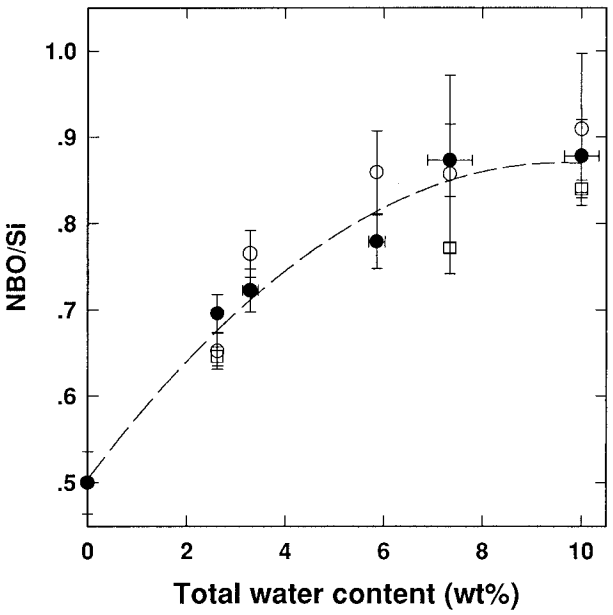

FIGURE 11. Dependence of the number of non-bridgingO atoms per silicon (NBO/Si) on the total water content: Raman data (empty circles); NMR data (empty squares); and near IR data (full circles). The dashed line is a polynomial fit through all the data points.

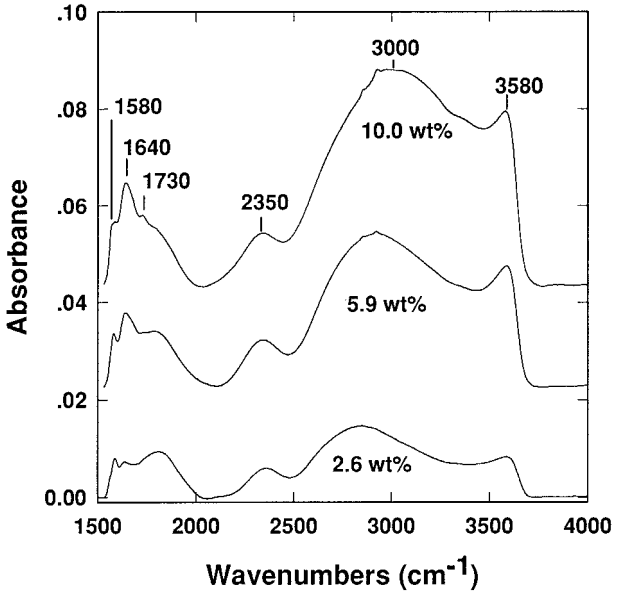

FIGURE 12. IR spectra of hydrous sodium tetrasilicate glasses in the OH stretching region (2000–4000 cm^{-1}). Spectra are offset by 0.02 absorbance units for clarity. All spectra are normalized to 450 μm thickness.

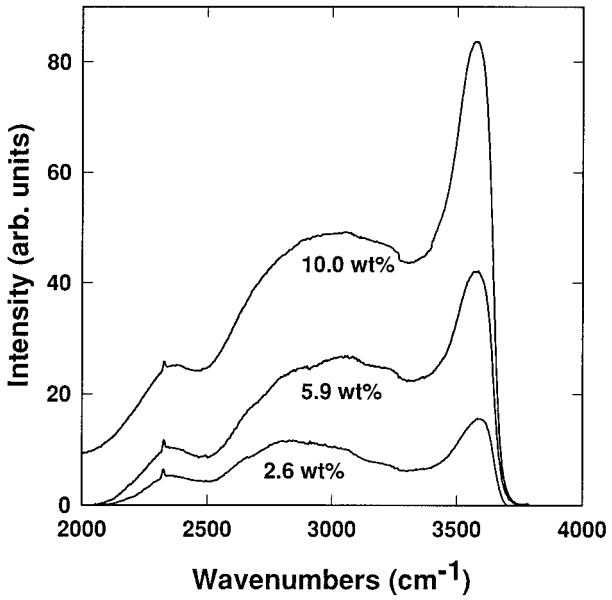

FIGURE 13. Unpolarized Raman spectra of hydrous sodium tetrasilicate glasses in the OH stretching region (2000–4000 cm^{-1}). The sharp feature at about 2325 cm^{-1} is due to N_2 in the air.

The decrease of isotopic shift with decreasing stretching frequency is again a result of increasing hydrogen bonding (Novak 1974).

The mid-IR spectra of hydrous sodium tetrasilicate glasses show much more structure than those of aluminosilicate compositions (e.g., Stolper 1982), which usually consist of only one broad asymmetric band without fine structure. It is therefore tempting to assign individual components in the OH-fundamental region either to OH groups or to molecular H_2O (e.g., Scholze 1959). However, a close inspection of the data in Figures 10, 12, and 13 show that this is probably not possible. The relative intensities of the three fundamental bands in the Raman and mid-IR spectra (Figs. 12 and 13) are essentially independent of total water content. This is already obvious from a brief visual inspection of the spectra and was confirmed by a quantitative decomposition into Gaussian components. In contrast, the ratio of OH groups to molecular water, as seen from the near IR data (Table 3 and Fig. 10), varies by about an order of magnitude over the studied concentration range. This would suggest that both molecular H_2O and OH groups contribute to each peak in the fundamental stretching region, or in other words, the presence of strong hydrogen bonding is unrelated to the relative proportions of H_2O and OH. This idea is consistent with the fine structure of the H_2O bending mode around 1600 cm^{-1} in the mid-IR spectra (Fig. 12). Three components are resolved at 1580, 1640, and 1730 cm^{-1}, possibly corresponding to the three main bands in the stretching region. Hydrogen bonding is well-known to shift the frequency of the H_2O bending mode to higher frequencies (Pimental and McClellan 1960). However, the bending modes in the glass spectra are superimposed on some broad features arising from overtones of the Si-O stretching fundamentals, which makes a quantitative deconvolution of the spectra difficult.

The most difficult question concerning the structure of

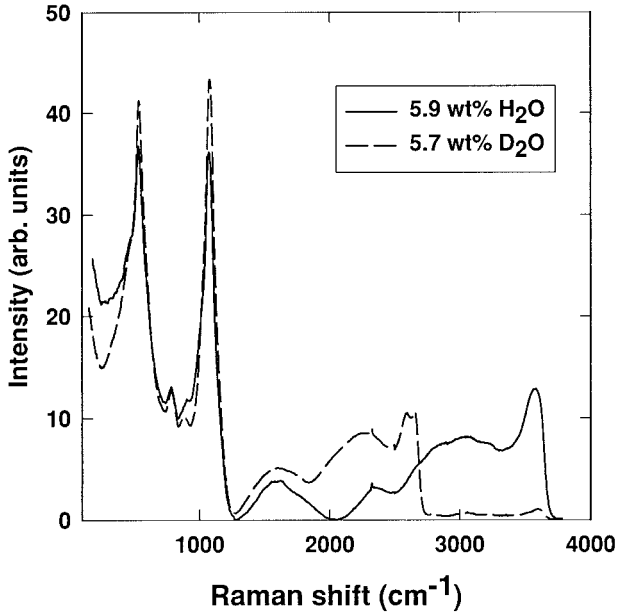

FIGURE 14. Unpolarized Raman spectra of the hydrous sodium tetrasilicate glass with 5.9 wt% H_2O and the deuterated glass with 5.7 wt% D_2O. The two spectra are normalized so that the area of both curves in the range 150–1300 cm^{-1} is the same.

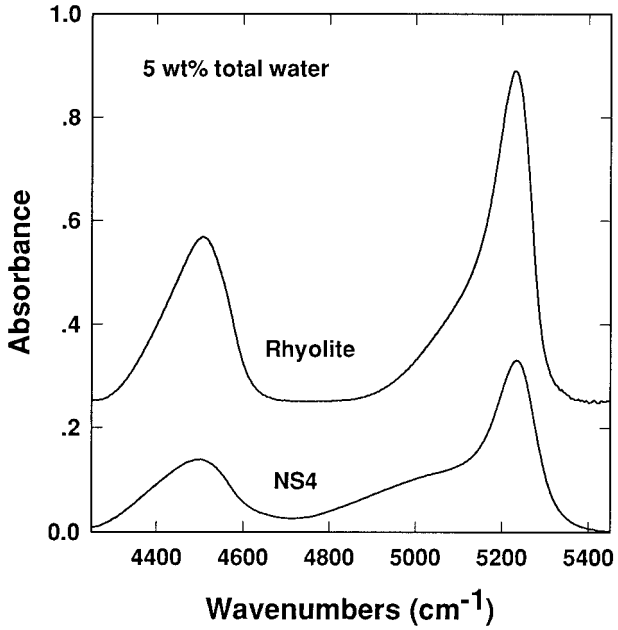

FIGURE 15. Near IR spectra of synthetic, iron-free rhyolite glass and of sodium tetrasilicate glass (NS4). Total water content in both samples 5 wt%, spectra normalized to 1 mm thickness.

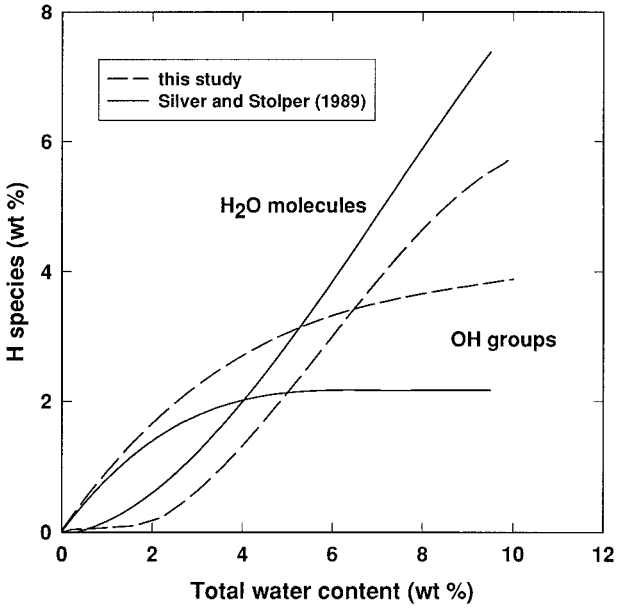

FIGURE 16. Water speciation in albite glass (redrawn from Silver and Stolper 1989) and in sodium tetrasilicate glass (this study).

hydrous glasses is related to the spatial distribution and possible clustering of OH and H_2O in the matrix (e.g., Stolper 1982; Eckert et al. 1987). In our recent neutron diffraction study of hydrous tetrasilicate glasses (Zotov et al. 1996), we were able to determine the hydrogen first-order difference correlation function $\Delta G_H(r)$ for the hydrous sodium tetrasilicate glass with 10 wt% total water by isotopic substitution. $\Delta G_H(r)$ represents the sum of all H-involved pair correlation functions. The absence of H···H and H···O distances characteristic for liquid water in $\Delta G_H(r)$ shows that ''micropools'' or ''microinclusions'' of molecular H_2O with a liquid-like structure do not exist in the glass. However, the changes observed by neutron diffraction in the first coordination shell of Na^+ would be consistent with the formation of a hydration shell of H_2O molecules around this ion, although the evidence is not conclusive. Water molecules surrounding alkali ions occur in the minerals analcime and pollucite. Interestingly, the stretching frequency of the water molecules in these minerals is at about 3620 cm^{-1} (Farmer 1974), very close to the 3580 cm^{-1} band observed in the hydrous sodium tetrasilicate glasses. Finally, a combination of ^1H relaxational NMR and two-dimensional ^1H spin-exchange NMR experiments suggest that in the hydrous sodium tetrasilicate glass with 4 wt% total water, the arrangement of the Si-OH and the H_2O species in clusters containing solely H_2O or solely Si-OH is very unlikely (Schaller and Sebald 1995).

Comparison with hydrous aluminosilicate glasses

All spectroscopic results presented here were obtained on hydrous sodium tetrasilicate glass and as such are not directly applicable to the more complex aluminosilicate systems. However, the near IR spectra of hydrous aluminosilicate glasses is strikingly similar to that of sodium tetrasilicate glass (Fig. 15). In our study we have shown beyond any reasonable doubt that the 4500 cm^{-1} band in the hydrous sodium tetrasilicate glass is due to Si-OH groups. However, it has been suggested that hydrous albite glass and similar aluminosilicate glasses do not contain appreciable amounts of Si-OH or Al-OH (Kohn et al. 1989). This is difficult to reconcile with the appearance of a band at 4500 cm^{-1} in the near IR spectra of these glasses, with virtually the same position, shape, width, and similar extinction coefficient as in sodium tetrasilicate glass. This problem becomes even more obvious if one compares the evolution of OH and H_2O species concentration with total water content, as derived from the intensities of the 4500 and 5200 cm^{-1} bands. Figure 16 shows that these curves are rather similar for hydrous albite and sodium tetrasilicate glass, suggesting a generally similar dissolution mechanism of water, involving formation of Si-OH or Al-OH groups and depolymerization of the glass structure.

Acknowledgments

We thank Torsten Schaller for measuring the ^{29}Si NMR spectra and discussing the results with us, Anna Dietel for ICP analyses, and Hubert Schulze for sample preparation. John Sowerby kindly provided the near IR spectrum of hydrous rhyolite glass. This work was supported by German Science Foundation (DFG, Ke 501/2-1).

References cited

Acocella, J., Tomozawa, M., and Watson, E.B. (1984) The nature of dissolved water in sodium silicate glasses and its effect on various properties. Journal of Non-Crystaline Solids, 65, 355–372.

Bartholomew, R.F., Butler, B.L., Hoover, H.L., and Wu, C.K. (1980) Infrared spectra of water-containing glass. Journal of the American Ceramic Society, 63, 481–485.

Behrens, H., Romano, C., Nowak, M., Holtz, F., and Dingwell, D.B. (1996) Near-IR spectroscopic determination of water species in glasses of the system $MAlSi_3O_8$ (M = Li, Na, K): an interlaboratory study. Chemical Geology, 128, 41–63.

Brawer, S.A. and White, W.B. (1975) Raman spectroscopic investigation of the structure of silicate glasses. I. The binary alkali silicates. Journal of Chemical Physics, 63, 2421–2432.

Buback, M., Crerar, D.A., and Vogel Koplitz, L.M. (1987) Vibrational and electronic spectroscopy of hydrothermal systems. In G.C. Ulmer and H.L. Barnes, Eds., Hydrothermal Experimental Techniques, p. 333–359. Wiley, New York.

Burnham, C.W. (1979) The importance of volatile constituents. In H.S. Yoder, Ed., The Evolution of the Igneous Rocks, p. 439–482. Princeton University Press, New Jersey.

Dupree, R., Holland, D., McMillan, P.W., and Pettifer, R.F. (1984) The structure of soda-silica glasses: A MAS NMR study. Journal of Non-Crystalline Solids, 68, 399–410.

Emerson, J.F., Stallworth, P.E., and Bray, P.J. (1989) High-field ^{29}Si NMR of alkali silicate glasses. Journal of Non-Crystalline Solids, 113, 253–259.

Engelhardt, G. and Michel, D. (1987) High resolution solid state NMR of silicates and zeolithes. Wiley, New York.

Eckert, H., Yesinowski, J.P., Stolper, E.M., Stanton, T.R., and Holloway, J. (1987) The state of water in rhyolitic glasses. A deuterium NMR study. Journal of Non-Crystalline Solids, 93, 93–114.

Farmer, V.C. (1974) The infrared spectra of minerals. Mineralogical Society, London.

Farnan, I., Kohn, S.C., and Dupree, R. (1987) A study of the structural role of water in hydrous silica glass using cross-polarization magic angle spinning NMR. Geochimica et Cosmochimica Acta, 51, 2869–2873.

Furukawa, T., Fox, K.E., and White, W.B. (1981) Raman spectroscopic investigation of the structure of silicate glasses. III. Raman intensities and structural units in sodium silicate glasses. Journal of Chemical Physics, 75, 3226–3237.

Galeener, F.L. (1982) Planar rings in vitreous silica. Journal of Non-Crystalline Solids, 49, 53–62.

Holtz, F., Beny, J.M., Mysen, B.O., and Pichavant, M. (1996) High-temperature Raman spectroscopy of silicate and aluminosilicate hydrous glasses: Implications for water speciation. Chemical Geology, 128, 25–39.

Keppler, H. and Bagdassarov, N.S. (1993) High-temperature FTIR spectra of H_2O in rhyolite melt to 1300 °C. American Mineralogist, 78, 1324–1327.

Kohn, S.C., Dupree, R., and Smith, M.E. (1989) A multinuclear magnetic resonance study of the structure of hydrous albite glasses. Geochimica et Cosmochimica Acta, 53, 2925–2935.

Kubicki, J.D. and Sykes, D. (1993) Molecular orbital calculations of vibrations in three-membered aluminosilicate rings. Physics and Chemistry of Minerals, 19, 381–391.

Kümmerlen, J., Merwin, L.H., Sebald, A., and Keppler, H. (1992) Structural role of H_2O in sodium silicate glasses: results from ^{29}Si and ^{1}H NMR Spectroscopy. Journal of Physical Chemistry, 96, 6405–6410.

Langer, K. and Flörke, O.W. (1974) Near IR absorption spectra (4000–9000 cm^{-1}) of opals and the role of ''water'' in these $SiO_2 \cdot nH_2O$ minerals. Fortschritte der Mineralogie, 52, 17–51.

Long, D.A. (1977) Raman Spectroscopy. McGraw-Hill, New York.

Maekawa, H., Maekawa, T., Kawamura, K., and Yokokawa, T. (1991) The structural groups of alkali silicate glasses determined from ^{29}Si MAS-NMR. Journal of Non-Crystalline Solids, 127, 53–64.

Matson, D.W., Sharma, S.K., and Philpotts, J.A. (1983) The structure of high-silica alkali silicate glasses. A Raman spectroscopic investigation. Journal of Non-Crystalline Solids, 58, 323–352.

McMillan, P.F. (1984) Structural studies of silicate glasses and melts—applications and limitations of Raman spectroscopy. American Mineralogist, 69, 622–644.

———(1994) Water solubility and speciation models. In Mineralogical Society of America Reviews in Mineralogy, 30, 131–156.

McMillan, P.F., Poe, B.T., Stanton, T.R., and Remmele, R.L. (1993) A Raman spectroscopic study of H/D isotopically substituted hydrous alumosilicate glasses. Physics and Chemistry of Minerals, 19, 454–459.

Mysen, B.O. and Virgo, D. (1986) Volatiles in silicate melts at high pressure and temperature. 2. Water in melts along the join $NaAlO_2$-SiO_2 and a comparison of solubility mechanisms of water and fluorine. Chemical Geology, 57, 333–358.

Mysen, B.O., Virgo, D., Harrison, W.J., and Scarfe, C.M. (1980) Solubility mechanisms of H_2O in silicate melts at high pressures and temperatures: a Raman spectroscopic study. American Mineralogist, 65, 900–914.

Mysen, B.O., Finger, L.W., Virgo, D., and Seifert, F.A. (1982a) Curve-fitting of Raman spectra of silicate glasses. American Mineralogist, 67, 686–695.

Mysen, B.O., Virgo, D., and Seifert, F.A. (1982b) The structure of silicate melts: Implications for chemical and physical properties of natural magma. Reviews of Geophysics and Space Physics, 20, 353–383.

Nakamoto, K., Margoshes, M., and Rundle, R.E. (1955) Stretching frequencies as a function of distances in hydrogen bonds. Journal of the American Chemical Society, 77, 6480–6488.

Newton, M.D. and Gibbs, G.V. (1980) Ab initio calculated geometries and charge distribution for H_4SiO_4 and $H_6Si_2O_7$ compared with experimental values for silicates and siloxanes. Physics and Chemistry of Minerals, 6, 221–246.

Novak, A. (1974) Hydrogen bonding in solids. Correlation of spectroscopic and crystallographic data. Structure and Bonding, 18, 177–216.

Nowak, M. and Behrens, H. (1995) The speciation of water in haplogranitic glasses and melts determined by in situ near-IR spectroscopy. Geochimica et Cosmochimica Acta, 59, 3445–3450.

Paterson, M.S. (1982) The determination of hydroxyl by IR absorption in quartz, silicate glasses and similar materials. Bulletin de Minéralogie, 105, 20–29.

Pichavant, M., Holtz, F., and McMillan, P.F. (1992) Phase relations and compositional dependence of H_2O solubility in quartz-feldspar melts. Chemical Geology, 96, 303–319.

Pimental, G.C. and McClellan, A.L. (1960) The Hydrogen Bond. Freeman, San Francisco.

Schaller, T. and Sebald, A. (1995) One- and two-dimensional ^{1}H magic-angle spinning experiments on hydrous silicate glasses. Solid State Nuclear Magnetic Resonance, 5, 89–102.

Scherer, J.R. (1978) The vibrational spectroscopy of water. In R.J.H. Clark and R.E. Hesters, Eds., Advances in IR and Raman Spectroscopy, p. 149–216. Heyden, London.

Scholze, H. (1959) Der Einbau des Wasser in Gläsern. Glastechnische Berichte, 32, 81–88, 142–145, 278–281, 314–320, 381–386.

Shen, A. and Keppler, H. (1995) Infrared spectroscopy of hydrous silicate melts to 1000 °C and 10 kbar: Direct observation of H_2O speciation in a diamond-anvil cell. American Mineralogist, 80, 1335–1338.

Silver, L.A. and Stolper, E.M. (1989) Water in albitic glasses. Journal of Petrology, 30, 667–709.

Stolper, E.M. (1982) Water in silicate glasses: An IR Spectroscopic study. Contributions to Mineralogy and Petrology, 81, 1–17.

Sykes, D. and Kubicky, J.D. (1993) A model for H_2O solubility mechanisms in albite melts from infrared spectroscopy and molecular orbital calculations. Geochimica et Cosmochimica Acta, 57, 1039–1052.

Yanev, Y. and Zotov, N. (1996) Infrared spectra of water in volcanic glasses. Experiment in Geosciences, 5, 1–10.

Zotov, N. and Keppler, H. (1998) The structure of sodium tetrasilicate glass from neutron diffraction, reverse Monte Carlo simulations and Raman Spectroscopy. Physics and Chemistry of Minerals, 25, 259–267.

Zotov, N., Keppler, H., Hannon, A.C., and Soper, A.K. (1996) The effect of water on the structure of silicate glasses—A neutron diffraction study. Journal of Non-Crystalline Solids, 202, 153–163.

Zotov, N., Michailova, B., Marinov, M., and Konstantinov, L. (1993) Vibrational spectra of rings in silicate glasses-calculation on isolated structural units with topological disorder. Physica A, 201, 402–409.

Manuscript received September 9, 1997
Manuscript accepted February 10, 1998
Paper handled by Jonathan F. Stebbins